

The dynamics of acute malaria infections. I. Effect of the parasite's red blood cell preference

Rustom Antia*, Andrew Yates and Jacobus C. de Roode

Department of Biology, Emory University, Atlanta, GA 30322, USA

What determines the dynamics of parasite and anaemia during acute primary malaria infections? Why do some strains of malaria reach higher densities and cause greater anaemia than others? The conventional view is that the fastest replicating parasites reach the highest densities and cause the greatest loss of red blood cells (RBCs). Other current hypotheses suggest that the maximum parasite density is achieved by strains that either elicit the weakest immune responses or infect the youngest RBCs (reticulocytes). Yet another hypothesis is a simple resource limitation model where the peak parasite density and the maximum anaemia (percentage loss of RBCs) during the acute phase of infection equal the fraction of RBCs that the malaria parasite can infect. We discriminate between these hypotheses by developing a mathematical model of acute malaria infections and confronting it with experimental data from the rodent malaria parasite *Plasmodium chabaudi*. We show that the resource limitation model can explain the initial dynamics of infection of mice with different strains of this parasite. We further test the model by showing that without modification it closely reproduces the dynamics of competing strains in mixed infections of mice with these strains of *P. chabaudi*. Our results suggest that a simple resource limitation is capable of capturing the basic features of the dynamics of both parasite and RBC loss during acute malaria infections of mice with *P. chabaudi*, suggesting that it might be worth exploring if similar results might hold for other acute malaria infections, including those of humans.

Keywords: mathematical model; malaria; resource limitation; competition; mixed infection

1. INTRODUCTION

Many aspects of malaria, and particularly the interactions between the parasite and its host which result in the disease, are still poorly understood (Miller *et al.* 2002). A malaria infection starts with the bite of an infected mosquito, which introduces a few sporozoite stages that migrate to and infect liver cells. Asexual replication in the liver cell results in the release of thousands of merozoites that initiate the blood stage of the infection. This stage is responsible for the pathology associated with malaria (anaemia, fever, cerebral malaria and coma). Merozoites infect red blood cells (RBCs) where they multiply to produce 8–32 new merozoites (depending on the malaria species), which are released by lysis of the RBCs. The released merozoites can infect new RBCs, causing a rapid increase in parasites and the infected cells. In this paper, we focus on the initial dynamics of infection of the merozoite stage of infection of naive hosts (individuals who have never had a previous malaria infection). This corresponds to the first week or the second following infection when the parasite density reaches a peak and the anaemia (loss of RBCs) may be severe.

During this initial or acute phase of infection, different parasite strains reach different densities and cause varying degrees of anaemia and other pathology (Field & Niven 1937; Field 1949; Kitchen 1949a; Molineaux *et al.* 2001; Mackinnon & Read 2004). While most studies agree that specific immunity does not play a major role in this initial dynamics, there is considerable controversy over which factors drive the dynamics shortly after infection

(Anderson *et al.* 1989; Hellriegel 1992; Hetzel & Anderson 1996; McQueen & McKenzie 2004). Some of the hypotheses to explain the differences in the initial dynamics of malaria strains include (i) the conventional view—in both the virulence evolution and the malaria literature—that the fastest replicating parasites reach the highest densities and cause most anaemia (Antia *et al.* 1994; Mason *et al.* 1999; Chotivanich *et al.* 2000; Gandon *et al.* 2001), (ii) the hypothesis that strains infecting reticulocytes (the youngest RBCs) cause the severest anaemia (McQueen & McKenzie 2004, 2006), and (iii) the hypothesis that innate or early specific immune responses regulate the initial dynamics of infection and anaemia (Jakeman *et al.* 1999; Haydon *et al.* 2003; Dietz *et al.* 2006).

There are two reasons why it is difficult to determine the contribution of these different factors to the dynamics of acute infection. The first problem is that there is relatively limited data on the dynamics of the parasite and the loss of RBCs following infection of humans with human malaria parasites such as *Plasmodium falciparum* and *Plasmodium vivax*. One approach to overcome this limitation is to use data from well-characterized model systems such as infections of mice with species such as *Plasmodium chabaudi* or *Plasmodium yoelii*. The second problem is that the dynamics of infection may involve many interacting populations which fall into three groups: (i) the parasite and its resource, i.e. merozoites, uninfected and infected RBCs, (ii) the innate immune response, i.e. macrophages, dendritic cells, cytokines, etc., and (iii) the adaptive immune response, i.e. B and T cells and antibodies. One approach to this problem is to start with

* Author for correspondence (rustom.antia@emory.edu).

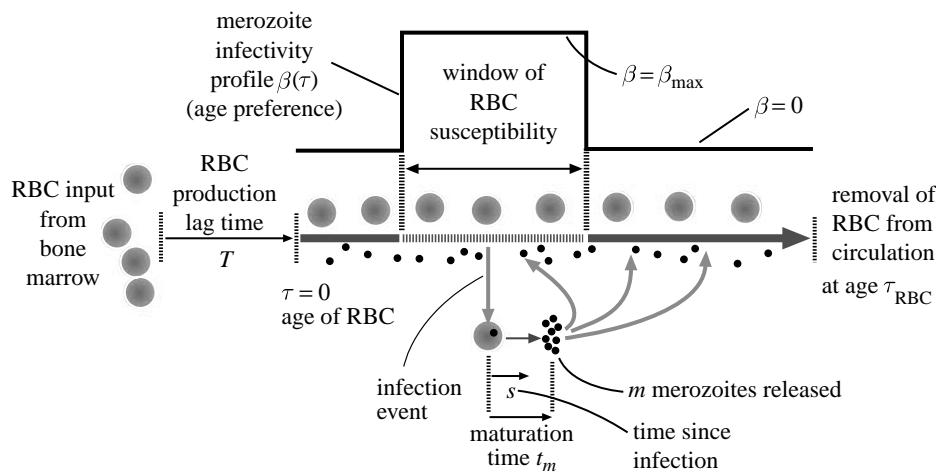


Figure 1. The model for the interaction between merozoites, uninfected and infected RBCs. The model accounts for (i) RBC production, regulation and lifespan, τ_{RBC} , (ii) the age-dependent force of infection of RBCs by merozoites, β , and (iii) the production of m new merozoites from infected RBCs after a maturation time, t_m . See the appendix for details.

the simplest possible mathematical model of the dynamics of infection (i.e. one that consists of simply the parasite and the uninfected and infected RBCs) and by confronting the model with the experimental data to determine which features of the infection the model can explain. Importantly, identifying where and how the model fails can help us determine how the model needs to be refined in future studies. This approach is similar to that used to dissect the early dynamics of infections such as HIV and influenza (Phillips 1996; Perelson 2002; Regoes *et al.* 2004; Baccam *et al.* 2006).

In this study, we bring mathematical models of the early stages of malaria infection into contact with detailed experimental data on the time-course of both the parasite density and the loss of RBCs following infection. We used data from infections of C57BL/6 mice with two strains of *P. chabaudi* (De Roode *et al.* 2004, 2005a,b) as shown in figure 2. The two parasite strains reach different maximum densities and cause different levels of anaemia—with strain AJ reaching higher densities and causing greater anaemia than strain AS. An examination of these data suggests immediately that the differences in the dynamics of infection cannot be accounted for by differences in the growth rates (defined as the initial exponential rate of growth) as the growth rates of the two strains are not statistically different ($p > 0.05$). The next step is to develop a simple ‘resource-limitation’ model to describe the dynamics of infection of mice with the AS and AJ parasite strains and to identify the properties of these strains which account for the difference in their dynamics. We then test our conclusions by determining whether our model with parameters from the single-strain infections can describe the dynamics of co-infection of mice with both the strains.

2. RESULTS

We use an age-structured model of the dynamics of parasites and RBCs (figure 1 and the appendix). We combine the age-structured model for RBCs described by Mackey (1996) with the model of the infection process along the lines of McQueen & McKenzie (2004). A key component in the model is that merozoites may preferentially infect RBCs of different ages as described by an

age-dependent force of infection $\beta(\tau)$. The infected RBCs lyse after t_m days to produce m merozoites/infected RBC.

We have independent estimates of all of the parameters of the model except $\beta(\tau)$ from the literature (table 1). The terms and parameters for RBC homeostasis were obtained from Mary *et al.* (1980) and Mackey (1996), and for the life cycle of infected RBCs from Cox (1988) and de Roode (2005).

We briefly outline how we infer the age preference of merozoites for RBCs, $\beta(\tau)$, from the data on dynamics of single infections; the details are given in the appendix. As a first approximation, we take $\beta(\tau)$ to be constant within some range and zero outside it, as shown in figure 1. We thus need to estimate three parameters, namely β_{max} and the youngest and oldest ages of RBCs that are susceptible. Given the maturation time of infected RBCs, t_m , and the number of merozoites produced per RBC, m , for the model to explain the rapid exponential growth, the infection process must be highly efficient (i.e. β_{max} must be sufficiently large that at the beginning of the infection almost all free merozoites infect susceptible RBCs before they are cleared). This provides a lower bound for β_{max} (and we show that our results are not very sensitive to its precise value provided it is above this bound). The next step is to estimate the age range of susceptible RBCs. Given that β_{max} is high, almost all susceptible RBCs are infected and killed, and the maximum level of anaemia equals the proportion of the RBC population that is susceptible to infection, σ . We estimated the fraction of RBCs that can be infected by the AJ and AS strains, $\sigma_{\text{AJ}} \approx 0.8$ and $\sigma_{\text{AS}} \approx 0.5$. The beginning of the age range can be estimated as follows: the time between maximum anaemia (approx. day 9) and the beginning of the second peak of parasitaemia (approx. day 24 for AS and approx. day 20 for AJ from (de Roode *et al.* 2005a) figure 3 single infections) is the time required for new target cells to appear. This is roughly the sum of the time lag associated with increased RBC production (2.5 days) and the time taken for these newly produced RBCs to enter the susceptible age range (τ_{min}). We thus obtain the age ranges for AJ as being 0.2–1.0 and AS being 0.4–0.9. These figures are in units of the average lifetime of RBCs, which is 40 days in mice. In other words, AJ is able to infect a wider range of RBCs than AS, and the age

Table 1. Parameter estimates. (Most of the parameters of the model have been obtained from the literature. The parameter β describing infectivity is obtained as described in the text and the appendix. The initial density of AS and AJ parasites was 10 each for the single infections and 10 of both for the multiple infections.)

parameter	meaning	value	references
m	mean number of merozoites produced per cell	8	Cox (1988) and de Roode (2005)
t_m	maturation time of infected RBC	approx. 1 day	Cox (1988) and de Roode (2005)
T	delay in RBC production feedback (approximately transit time in bone marrow)	2.5 days	Mary <i>et al.</i> (1980)
F_0	max. RBC production rate/ μl day	9.1×10^5	Mackey (1996)
θ	RBC count/ μl at which production is half-maximum	7.3×10^6	Mackey (1996)
κ	Hill exponent of RBC production feedback function	7.6	Mackey (1996)
τ_{RBC}	mean RBC lifetime in mice	40 days	Bannerman (1983)
d_m	inverse of free merozoite lifetime	48 d^{-1}	Garnham (1966)
$\beta(\tau)$	infectivity as function of RBC age τ		
β_{max}	max. value of $\beta(\tau)$	5×10^{-5}	
<i>infectivity profile for AS</i>			
τ_{min}	age of the youngest susceptible RBCs	12 days	
σ	fraction of RBCs that are susceptible	0.5	
<i>infectivity profile for AJ</i>			
τ_{min}	age of the youngest susceptible RBCs	8 days	
σ	fraction of RBCs that are susceptible	0.8	

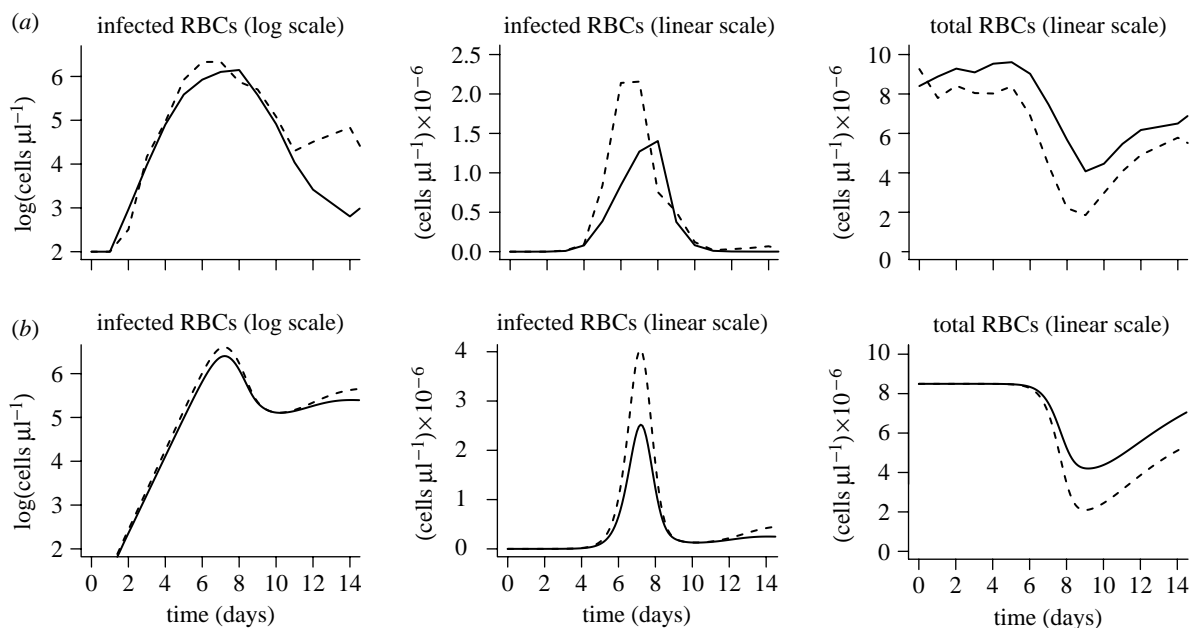


Figure 2. (a) Experimental data and (b) simulations for single-strain infections. The dynamics of the infections with either AS (solid line) or AJ (dashed line) parasites. Plots show the parasite density (described by the numbers of infected cells) as well as the total number of RBCs (their loss is a measure of virulence) as a function of time since infection. The simulations describe the experimental data on the dynamics of the first wave of parasitaemia, and the loss of RBCs. After approximately 12 days, when acquired immunity is expected to kick in, the simulations begin to depart from the experimental data.

preference of AS is contained entirely within that of AJ, i.e. AJ can infect both younger and older cells than AS.

In figure 2, we show that the model with these parameter estimates captures the key features of the experimental data of the dynamics of single-strain infections over the first 10–12 days of infection; the two strains have indistinguishable growth rates, but reach different peak levels and induce different degrees of anaemia. The simulations also reproduce the observed delays between the peak in parasite density and the time of maximum anaemia. Following the end of the second week of the infection, the results of the simulations depart from

the data. These observations can be explained using knowledge of the underlying biology and simple analytical calculations.

During the initial growth phase, the number of infected cells $Y(t)$ increases exponentially as $Y(t) \approx Y_0 m^{t/t_m}$. This is simply understood as follows: a single infected cell produces m merozoites after a time t_m and, at the onset of infection, target cells are in excess and essentially all merozoites produced go on to productively infect RBCs. This explains why the initial growth rate depends only on these two parameters, which are similar for AS and AJ, and not on the infectivity profile $\beta(\tau)$, which differs for AS and AJ.

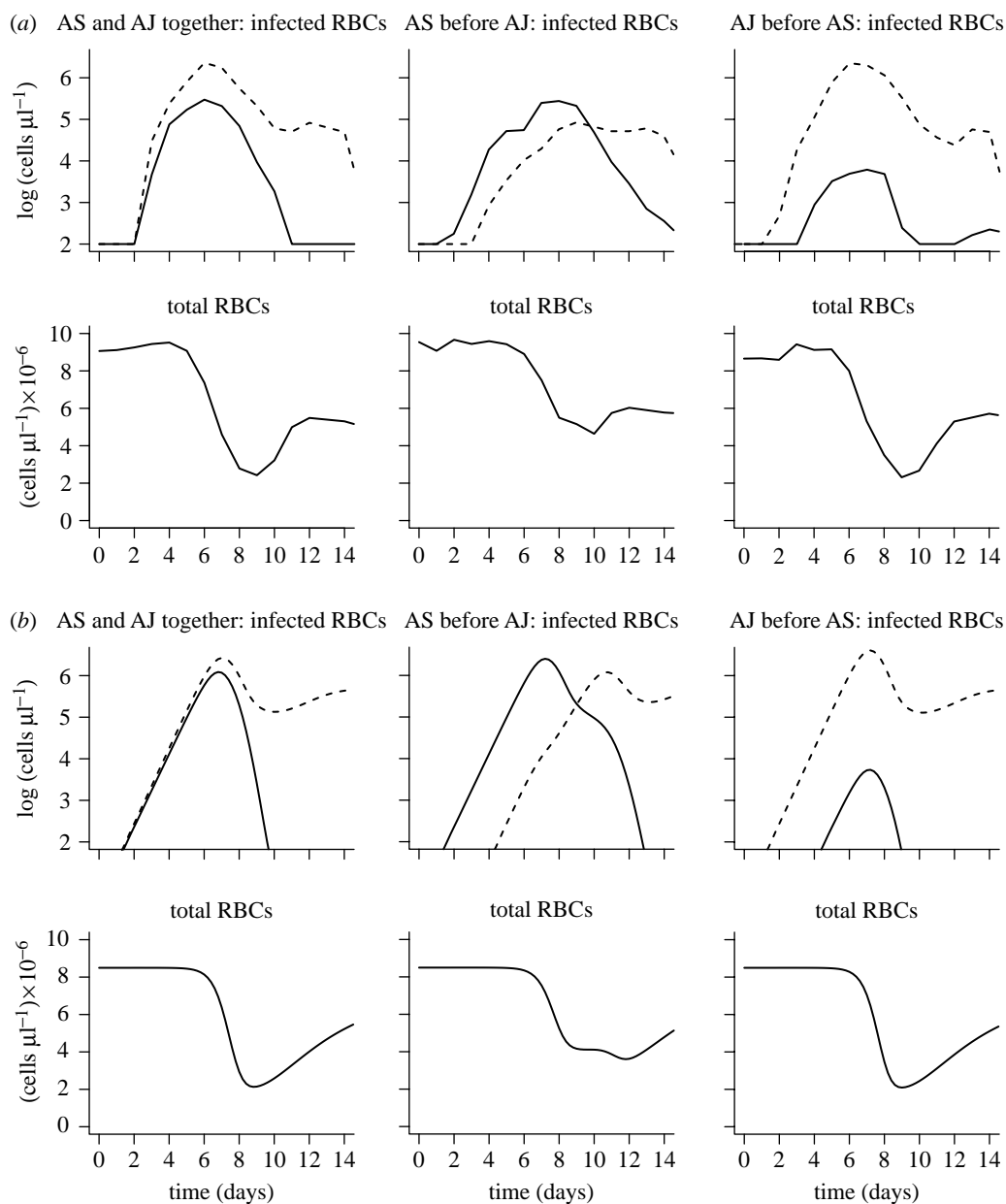


Figure 3. (a) Experimental data and (b) simulations for mixed infections. The dynamics of infection with both AS (solid line) and AJ (dashed line) parasites following either simultaneous infection or infection with one parasite strain 3 days prior to the other. Plots show the parasite density of the individual strains and the total number of RBCs as a function of time since infection. The simulations describe the experimental data on the dynamics of the first wave of parasitaemia, and the loss of RBCs. After about 12 days, when acquired immunity is expected to play an important role, the simulations begin to depart from the experimental data.

The model not only accurately describes the initial growth rate of the parasite but also the peak parasite density and the minimum RBC density, suggesting that RBC limitation is sufficient to explain the key features of the initial dynamics, and that differences in the age range of RBCs that are susceptible to infection can account for the differences in the dynamics of the two clones. In the appendix we show that the peak parasite density and the maximum anaemia are linearly dependent on the width, σ , of the age range of RBCs that are susceptible to infection.

We observe that the model begins to fail subsequent to day 12 after infection. Following this time, the parasite density drops to a lower level than predicted by the simulations. This suggests that immunity plays an important role in controlling the parasite after this time.

This is consistent with the experimental observations of the presence of parasite-specific antibodies beginning at approximately two weeks after infection (Mota *et al.* 1998).

The next step is to test or validate our model. We do so by asking whether without any modification it can reproduce the dynamics of competing strains in mixed infections. In other words, we used the parameters we have obtained for AS and AJ and change only the initial conditions to simulate the introduction of the two strains at the appropriate times. Figure 3 shows that the model agrees closely with all the mixed infection data. In particular, in simultaneous infections of AS and AJ parasites, the density of both initial peaks is somewhat lower than that in single-strain infections and AJ

subsequently outcompetes AS. When AS is introduced 3 days before AJ, the initial peak of AS is higher than that of AJ, but AJ invades and takes over and AS is not seen subsequently. The results also show that the duration of anaemia is substantially extended. Finally, following the introduction of AJ 3 days prior to AS, the initial peak of AJ is not substantially altered by AS, and AS has only a small primary peak several logs lower than that during single-strain infection and it is subsequently eliminated by AJ. The anaemia is similar to that of the infection with AJ alone. As in the case for infections with a single parasite strain, the onset of humoral immunity at day 12 results in the simulations departing from the data after this time.

3. DISCUSSION

Our results suggest that the dynamics of parasites and the loss of RBCs during the initial acute stages of *P. chabaudi* infections can be understood in terms of a simple resource limitation model with the RBCs as the resource for the parasite. The differences in the dynamics of the parasite and the loss of RBCs following infection with different (AS and AJ) strains of *P. chabaudi* can be explained by the differences in the age preferences of the parasite strains.

We developed this model based on the data for the densities of parasites and RBCs following infection of mice with a single parasite strain. We tested this model by showing that it could describe the dynamics of competition following co-infections with both strains under a number of different conditions. For simultaneous co-infection, we found that since the two strains' age preferences overlap, in the first peak of infected RBCs the density of each parasite is lower than that in a single-strain infection. As new RBCs are produced, AS is outcompeted as its potential target RBCs are infected by AJ before AS parasites can infect them. In mice infected with AS first, anaemia is extended as there are effectively two waves of depletion (AS induces a 50% anaemia, which is prolonged by the depletion induced by AJ peaking 3 days later and infecting a wider range of RBCs). In mice infected with AJ first, AS target cells are substantially depleted by the time AS is introduced and infection dynamics are similar to those of AJ alone. The model thus provides an explanation for the observed correlation between virulence and competitive ability in mixed infections with the AS and AJ strains (de Roode *et al.* 2005a; Bell *et al.* 2006). In ecological terms, the extent of competition depends on the degree to which the different populations share resources, and strains with a larger resource (RBC age range) are less affected by a resource loss due to competing strains.

Thus far, we have considered the dynamics of the AS and AJ strains, which have the same growth rate. In the appendix, we use our model to explore how the initial growth rate of strains affects their dynamics in single and mixed infections. For the case of single-strain infections, we find that our principal result, namely that the age preference determines the maximum parasite density and maximum loss of RBCs, holds independent of the growth rate of the strain. For the case of multiple-strain infections, we find that the extent of competition is dependent on the overlap in the age preference of the two strains for RBCs

and that strains with a higher growth rate and a wider age preference for RBCs have a competitive advantage.

We now consider the previous hypotheses for the dynamics of the parasite and the loss of RBCs during malaria infections. We have shown that the maximum parasite density and anaemia are insensitive to the initial growth rate (which affects the time of the peak but not its magnitude), rejecting the hypothesis that virulence is proportional to the initial multiplication rate (Antia *et al.* 1994; Mason *et al.* 1999; Chotivanich *et al.* 2000; Gandon *et al.* 2001). We also describe the dynamics of RBCs entirely as a consequence of loss following infection by merozoites. This suggests that the role of bystander destruction of uninfected RBCs (Jakeman *et al.* 1999; Haydon *et al.* 2003) may need to be reconsidered, at least for the initial dynamics of *P. chabaudi* infections of mice.

Many models have indicated the importance of RBC limitation (Anderson *et al.* 1989; Hellriegel 1992; Gravenor *et al.* 1995; Hetzel & Anderson 1996; Mason *et al.* 1999; Haydon *et al.* 2003) but are not able to explain the observation that strains with identical growth rates generate different parasite densities and hence different degrees of anaemia. The need to consider the RBC age preference to explain infection dynamics has been emphasized in the modelling studies of McQueen & McKenzie (2004, 2006). However, they suggested that following infection with a single parasite species, the extent of anaemia depends on the youngest age of RBCs that the strain infects. This is because in the absence of immunity, the killing of young cells induces greater anaemia, owing to the downstream impact on the RBC age profile. However, our study suggests that this does not happen in the *P. chabaudi* infections modelled here because immunity must be considered shortly after the peak in parasite density and this limits the subsequent aggravation of anaemia predicted by these models.

Our model is more parsimonious than others that invoke innate or specific immunity (Dietz *et al.* 2006) as it does not involve an additional term for innate immunity. More work will need to be done in order to determine the relative contributions of RBC limitation and innate immunity. At present, there are a number of difficulties with modelling the innate immunity, including the lack of quantitative measurements of the magnitude of innate immunity and uncertainty in the term for the killing of merozoites and infected cells by innate immunity.

Finally, we note that the observation that the model begins to fail after 12 days post-infection suggests a role for specific immune responses arising at this time. This is the time at which antibody responses develop in mice (Mota *et al.* 1998). Models considering the dynamics following this time will need to explicitly consider the effects of the adaptive immune responses of the host and antigenic variation of the parasite (Frank 1999; Recker *et al.* 2004). This is, however, beyond the scope of the current paper, which focuses on the initial or acute stage following infection.

Because our model was based on data from rodent malaria, its key predictions can be subject to further experimental tests. The most important prediction concerns the age ranges of RBCs that different malaria strains can infect. These could be determined by transferring labelled RBCs of different ages into singly infected mice and determining their loss following infection. An indirect

approach would be to compare competition between malaria strains in untreated mice, and mice treated with erythropoietin (the hormone that stimulates erythropoiesis, the production of RBCs) just prior to infection (Suzuki *et al.* 2006). Specifically, we predict that such a treatment would result in an increase in the relative density of strains that can infect younger RBCs.

Several experimental and theoretical studies have suggested a role for RBC age preference in the dynamics of human malaria infections (Kitchen 1949b; Hutagalung *et al.* 1999; Simpson *et al.* 1999; Chotivanich *et al.* 2000; Miller *et al.* 2002; Duraisingh *et al.* 2003; McQueen & McKenzie 2004, 2006) as well as in the experimental *Plasmodium berghei* infections of mice (Cromer *et al.* 2006). For example, *P. falciparum* isolates able to invade a larger proportion of RBCs maintained higher parasitaemias and caused more disease (Simpson *et al.* 1999; Chotivanich *et al.* 2000); similarly, an aberrant red cell phenotype in haemoglobin E carriers resulted in a reduced number of suitable cells for parasite invasion (Chotivanich *et al.* 2002), and was associated with a lower incidence of severe malaria (Hutagalung *et al.* 1999). It has also been suggested that the difference in virulence between *P. vivax* (mild) and *P. falciparum* (virulent) in humans could be due to the latter's ability to invade a wider range of erythrocytes than the former (Kitchen 1949b; Simpson *et al.* 1999; Miller *et al.* 2002). There are a number of difficulties associated with linking our model with these observations regarding the dynamics of anaemia in humans. Our results describe the initial stages of untreated acute infections, and many, if not most, of the experimental studies mentioned above consider the dynamics of the parasite and the virulence it causes during the persistent phase of infection or possibly following reinfection of semi-immune hosts. In these circumstances, immunity and antigenic variation play a major role in determining the dynamics of the parasite (Phillips *et al.* 1997; Bruce *et al.* 2000; Bruce & Day 2002; Recker *et al.* 2004) and anaemia is likely to be multifactorial (Menendez *et al.* 2000).

In conclusion, we note that much remains to be done to extend the model of parasite and RBCs to incorporate factors such as immunity and antigenic variation. A key problem will be bringing the resulting models into close contact with experimental data in a way which allows the models to be tested. While this may be essential for understanding the complex dynamics of chronic infections and the pathology they cause, our results suggest that many features of acute malaria infections (at least in the *P. chabaudi* model system) can be explained by RBC age preference.

We thank S. Altizer, M. Choisy, J. Davies, A. Graham, G. Long, A. Read, A. Pedersen, P. Rohani and H. Wearing for their helpful comments and discussion. R.A. and A.Y. acknowledge support from the NIH, and J.d.R. acknowledges support from a Netherlands organization for scientific research (NWO) TALENT fellowship and a European Commission Marie Curie Outgoing International fellowship.

APPENDIX A

(a) Model

We use an age-structured model of the RBC dynamics that explicitly incorporates the well-defined lifetime of RBCs in the blood, the time delay between infection of a RBC and

its bursting to produce new merozoites and the delayed response of the haematopoietic system to anaemia induced by infection.

The model is described below. Here, $x(t, \tau)$ is the population density of uninfected RBCs of age τ (time since release into blood) at time t ; $y(t, \tau, s)$ is the population density of RBCs infected at age τ , at a time s since infection, at time t ; $z(t)$ is the density of free merozoites in the blood; $X(t)$ is the total number of uninfected RBCs in the blood; and $Y(t)$ is the total number of infected RBCs in the blood. All populations are measured in units of cells or merozoites per microlitre.

$$\frac{\partial x}{\partial t} + \frac{\partial x}{\partial \tau} = -\beta(\tau)x(t, \tau)z(t), \quad (\text{A } 1)$$

$$X(t) = \int_0^{\tau_{\text{RBC}}} x(t, \tau) d\tau, \quad (\text{A } 2)$$

$$x(t, 0) = F_0 \frac{\theta^\kappa}{\theta^\kappa + (X(t-T))^\kappa}, \quad (\text{A } 3)$$

$$\frac{\partial y}{\partial t} + \frac{\partial y}{\partial \tau} + \frac{\partial y}{\partial s} = 0, \quad (\text{A } 4)$$

$$y(t, \tau, s=0) = \beta(\tau)x(t, \tau)z(t), \quad (\text{A } 5)$$

$$Y(t) = \int_0^{t_m} ds \int_0^{\tau_{\text{RBC}}} d\tau y(t, \tau, s), \quad (\text{A } 6)$$

$$\begin{aligned} \frac{dz(t)}{dt} = & -d_m z(t) + m \int_{\tau=0}^{\tau_{\text{RBC}}} y(t, \tau, s=t_m) d\tau \\ & - z(t) \int_{\tau=0}^{\tau_{\text{RBC}}} \int_{s=0}^{t_m} \beta(\tau)(x(t, \tau) + y(t, \tau, s)) d\tau ds. \end{aligned} \quad (\text{A } 7)$$

When solving these equations to generate the simulations, we break the age ranges of healthy and infected RBCs into compartments, generating sets of coupled ordinary differential equations (ODEs). By taking this computationally more tractable approach, we switch from a model of fixed, constant RBC lifetimes and infected cell maturation times (the partial differential equation system above) to a 'mean-field' model of the dynamics of the expected total cell numbers, where individual RBC lifespans and infected cell maturation times are gamma distributed (with means τ_{RBC} and t_m , respectively) and with variance decreasing as we increase the number of compartments. In this ODE framework, the RBC production delay T is simulated by introducing a series of transit compartments before release into the blood. The simulations were run as sets of coupled ODEs, with 10 compartments each for the delay in RBC production, the age structure of RBCs and infected RBCs.

(b) Estimating parameters

(i) Invariance of growth rate

Our model describes the initial growth rates of the AS and AJ strains, and explains why these growth rates are similar. Assume that we start with a population density $x(t=0, \tau) = x_0(\tau)$ of target RBCs. After t_m days (the maturation time), each infected cell bursts to give m merozoites, which die or are cleared from the blood at rate $d_m d^{-1}$ or can then go on to infect other cells. If $\beta(\tau)$ is the age-dependent infectivity of the strain, the following fraction of these merozoites goes on to infect

other cells:

$$\eta = \frac{\int \beta(\tau)x_0(\tau) d\tau}{\int \beta(\tau)x_0(\tau) d\tau + d_m} = \frac{\int \beta x_0 d\tau}{\int \beta x_0 d\tau + d_m}, \quad (\text{A } 8)$$

where from here on we drop the explicit age dependence when writing $\beta(\tau)$ and $x_0(\tau)$. The quantity η can be thought of as the ‘efficiency’ of infection. We can write the growth of infected cells as

$$Y(t) = (m\eta)Y(t - t_m). \quad (\text{A } 9)$$

Therefore, the growth of the number of infected RBCs $Y(t)$ goes as

$$Y(t) \sim (m\eta)^{t/t_m}, \quad (\text{A } 10)$$

or

$$\frac{\log Y(t)}{t} = g = \frac{\log(m\eta)}{t_m}. \quad (\text{A } 11)$$

This gradient g is the slope of the regression of $\log(Y(t))$ against time shortly after infection in [figure 2a,b](#). The rate g is constant and close to unity for both AS and AJ. Equations (A 8) and (A 11) give

$$\frac{d_m}{\int \beta x_0 d\tau} = \frac{m}{10^{gt_m}} - 1. \quad (\text{A } 12)$$

This allows us to constrain the value of $d_m/\int \beta x_0 d\tau$ given a value of the infected cell maturation time t_m . The estimates of t_m are approximately 1 day, implying $d_m/\int \beta X_0 d\tau \ll 1$. This suggests that during the exponential growth of the infected cells, infection is very efficient ($\eta \approx 1$) and effectively all merozoites produced go on to productively infect RBCs. From the definition of η (equation (A 8)), this implies that the growth rate is independent of the infectivity β provided the above inequality is satisfied. That is, the initial growth rate of parasites, when target cells are not limited, is likely to be the same for all strains even if they differ in their infectivities and age preferences.

(ii) *Estimating the age preferences of each strain from single infection data*

We suggest that the initial rate of growth of infection is independent of β and is purely a function of the maturation time t_m and the number of merozoites produced per infected cell, m . What can we infer from the size of the peak and anaemia produced by the infection? A simple intuitive picture suggests that the anaemia produced by the first wave of infection constrains the width of the age preference of merozoites for target cells. If a particular strain is able to infect a fraction σ of the RBC population, then if we ignore the influx from the bone marrow and ageing dynamics, we expect cell counts at the minimum to be a fraction $(1 - \sigma)$ of healthy numbers, as all target cells are exhausted. For AJ, we see a fall in the total RBC density from 9.3×10^6 to $1.9 \times 10^6 \mu\text{l}^{-1}$ at day 10, suggesting $\sigma_{\text{AJ}} \approx 0.8$. For AS, the cell densities fall from 8.4 to 4.1, giving $\sigma_{\text{AS}} \approx 0.5$.

We can obtain slightly more formal estimates as follows. At the peak, the growth rate of the infected cells passes through zero. That is, from equation (A 10)

$$\log(m\eta) = 0,$$

or

$$\frac{m}{1 + d_m/\int \beta(\tau)x(t, \tau) d\tau} = 1,$$

so that at the peak of infection

$$\frac{d_m}{\int \beta(\tau)x(t, \tau) d\tau} = m - 1 \approx 7.$$

Assume that the infectivity profile $\beta(\tau)$ is uniform—zero outside a fraction σ of the age range and β_{max} within it. Then

$$\int \beta(\tau)x(t, \tau) d\tau \equiv \beta_{\text{max}}X_{\text{susc}},$$

where X_{susc} is the number of cells that fall within the region σ (that is the number of susceptible cells remaining) at time t . At the beginning of the infection, $X_{\text{susc}} = \sigma X_0$, where X_0 is the total (healthy) RBC count. Our constraint from the estimates of the initial slope gives us

$$d_m \ll \beta_{\text{max}}\sigma X_0. \quad (\text{A } 13)$$

At the peak of infection, the total RBC count will be

$$X = X_{\text{susc}} + (1 - \sigma)X_0, \quad (\text{A } 14)$$

$$X = \frac{d_m}{7\beta_{\text{max}}} + (1 - \sigma)X_0, \quad (\text{A } 15)$$

$$X \approx (1 - \sigma)X_0, \quad (\text{A } 16)$$

where the last line uses equation (A 13), and we ignore the influx into the susceptible region from ageing of younger cells.

The finite maturation time of the infected cells imposes a delay between the point of maximum rate of infection and the resulting anaemia. Thus, we expect to see a minimum total RBC count of $(1 - \sigma)X_0$ approximately t_m after the peak in the infected cell numbers, or at around day 7.

As a further confirmation of this, we can calculate how well the model with a given age range of susceptible RBCs, σ , is able to fit the data on the numbers of RBCs. This has been shown in [figure 4](#). We note that (i) we fit the model until day 10 as we have shown that at later times immunity becomes important and (ii) the fits to the data on peak parasite density and anaemia for single-strain infections are insensitive to the second parameter t_1 , which determines whether young or old RBCs are preferentially infected (data not shown).

(iii) *Constraining age preferences*

The second peak arises as new target cells generated in response to the anaemia induced by the first peak become old enough to be infected by the parasite. Its timing contains information about the youngest age of RBCs that the strain can infect, τ_{min} . After the anaemia induced by the first wave of infection, it takes a delay of T days for a large cohort of new RBCs to be released into the blood and a further τ_{min} days for these cells to begin to enter the susceptible age range. That is, if t_1 and t_2 are the times of the first and second peaks, respectively, then

$$t_2 - t_1 \approx T + \tau_{\text{min}}. \quad (\text{A } 17)$$

Since we have estimates of T from the literature and the peak timings from the data, we can use the single infection data to estimate the τ_{min} for each strain.

(iv) *A more detailed infectivity profile $\beta(\tau)$*

At this stage, we do not know the shape of the infectivity age profile $\beta(\tau)$. In the absence of experimental data on the shape of the infectivity profile, we have assumed a simple

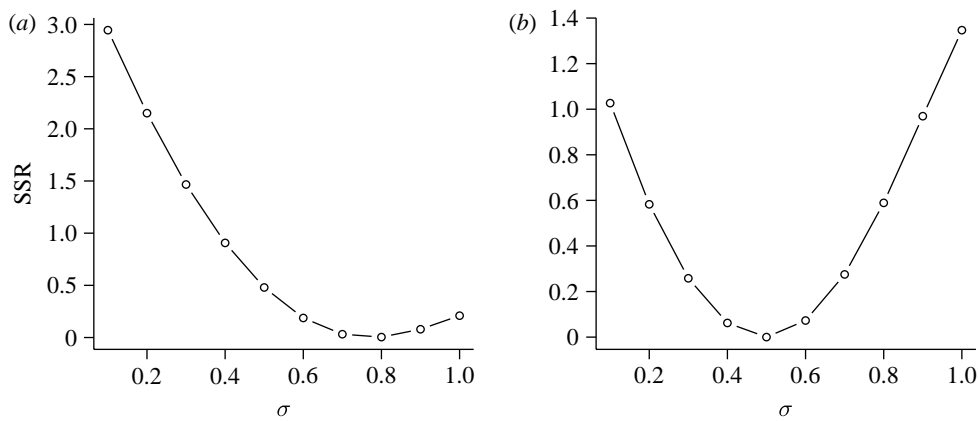


Figure 4. We show how well the model fits the data on anaemia (numbers of RBCs over time) for single-strain (a) AJ and (b) AS infections. We do so by plotting the sum of squared residuals (SSR) as a function of the fraction of RBC σ that the parasite can infect.

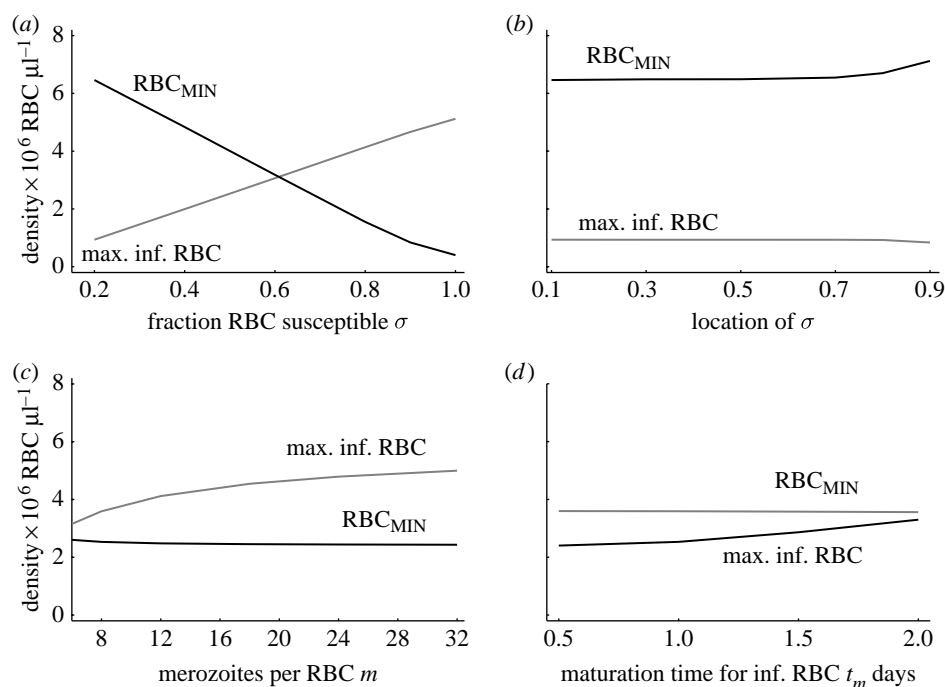


Figure 5. The dependence of peak parasite density and the minimum number of RBCs following single infections on parameters. (a) The peak parasite density and the loss of RBCs are linearly proportional to the fraction of RBCs that are susceptible to infection σ , but not on (b) whether young or old RBCs are susceptible. In (c,d), we show that the peak parasite density and the minimum number of RBCs do not depend on the parameters m and t_m which determine the initial growth rate of the parasite. Parameters as in table 1, $\sigma = 0.7$ (between 0.2 and 0.9). (a) Age range 0 to σ and (b) σ set at 0.2 and the location of the mean value changed from the youngest to the oldest age.

step function for $\beta(\tau)$. Our results suggest that AJ can infect approximately 80% of all RBCs, while AS can infect approximately 50% of RBCs. The next step is to experimentally test this prediction by transferring labelled RBCs of different ages into singly infected mice and determining their loss following infection. This will give us the precise shape of $\beta(\tau)$ for the different strains. This will allow us to check our prediction (that the width of $\beta(\tau)$ for the AJ strain is about 1.6 times as broad as that for the AS strain) and also gives us a better estimate of the shape of $\beta(\tau)$.

We have found that the basic results hold if we change the infectivity age profile $\beta(\tau)$ to a normal distribution or gamma distribution. We also note that we do not estimate the parameters by fitting the model to the entire dataset directly; since the model does not incorporate immunity, it diverges from the data after adaptive immune responses

are generated and this systematic bias would lead to incorrect parameter estimates. Once we have a clearer idea of the shape of $\beta(\tau)$ from the relevant experiments, incorporating this into the model will improve the fits of the model with the data.

(c) Generalizations

We have focused on explaining the dynamics of infections with the AJ and AS strains of malaria. These strains have similar parameters for the maturation time of an infected RBC t_m and the number of merozoites m produced following bursting of the RBC at this time. Here, we use the model to consider what would happen if these parameters can vary. In doing so, we examine in a general way the factors that affect the dynamics of parasites and the virulence during single- and multi-strain infections.

(i) *Single-strain infections*

The number of infected RBCs $Y(t)$ following infection with a single strain shortly after infection is described by equation (A 10):

$$Y(t) \sim Y(0)(m)^{t/t_m} = Y(0)e^{rt},$$

where r , the exponential growth rate shortly after infection, equals $\ln(m)/t_m$, provided the infection is relatively efficient (i.e. provided $d \ll \beta_{\max}\sigma X_0$).

- (i) In figure 5*a,b*, we see that the peak parasite density and the level of virulence (loss of RBCs), to a first approximation, depend linearly on the fraction of RBCs which the strain can infect (σ), but are relatively insensitive to where the age range of infectivity is located (i.e. whether the parasite can infect young or old RBCs). Provided the infectivity β_{\max} is high, as we expect to be the case (see discussion after equation (A 12)), the peak parasite density and virulence are independent of β_{\max} .
- (ii) In figure 5*c,d*, we see that the peak parasite density and the level of virulence (loss of RBCs) are relatively insensitive to the initial growth rate of the strain, which is independent of whether the initial growth rate is changed by changing the number of merozoites produced per RBC or the maturation time of infected RBCs. We note however that strains growing faster reach their peak parasite density earlier (results not shown).

The model thus makes quantitative predictions for how the parasite density and the loss of RBCs are related to the parameters describing the parasite life cycle, and its interactions with RBCs. Experimentally determining the dynamics of infections of parasites with different parameters (such as m , t_m and σ) will thus allow the model to be tested.

(ii) *Competition during co-infection*

We now consider how competition between different strains during acute infections depends on the age preference of RBCs which they can infect as well as the initial growth rate of the strains. We restrict consideration to the time-frame before the initiation of specific immune responses—after these are elicited, they play an important role in the control of the parasite (following approx. day 12 in *P. chabaudi* infections) and a purely resource-limited model is no longer valid.

We first consider how competition depends on the age preference of the two strains. During the initial phase of acute infections when the parasite densities are expanding exponentially, the extent of competition is largely limited to the extent to which their RBC age preferences overlap. In ecological terms, the extent of competition depends on the degree to which the different populations share resources. Following the peak in parasite densities as the densities fall, the strain that can infect younger RBCs has a competitive advantage. This happens because the strain that can infect younger RBCs gets access to RBCs as they are replenished which also results in a subsequent depletion of older RBCs. We note that resource competition lasts only a short time—between the time the parasites reach high densities and when the specific immune responses come into play.

We now consider competition between strains with different growth rates. If the strains are introduced

simultaneously (and at the same densities) the faster growing strain will use the shared resources faster, thus outcompeting the slower growing strain in mixed infections. This competitive advantage occurs even if the faster growing strain is introduced shortly after the slower growing strain, provided its higher growth rate allows it to reach its peak density before the slower growing strain reaches its peak density. The loss of RBCs during the course of mixed infections is then determined by the combined RBC age preference of the individual strains.

In summary, strains with a higher growth rate, a wider age preference for RBCs and an earlier age preference for RBCs will have a competitive advantage.

REFERENCES

- Anderson, R. M., May, R. M. & Gupta, S. 1989 Non-linear phenomena in host–parasite interactions. *Parasitology* **99**(Suppl.), S59–S79.
- Antia, R., Levin, B. R. & May, R. M. 1994 Within-host population dynamics and the evolution and maintenance of microparasite virulence. *Am. Nat.* **144**, 457–472. (doi:10.1086/285686)
- Baccam, P., Beauchemin, C., Macken, C. A., Hayden, F. G. & Perelson, A. S. 2006 Kinetics of influenza A virus infection in humans. *J. Virol.* **80**, 7590–7599. (doi:10.1128/JVI.01623-05)
- Bannerman, R. M. 1983 Hematology. In *The mouse in biomedical research*, vol. III, ch.12. *Normative biology, immunology, and husbandry* (eds J. D. Small, H. L. Foster & J. G. Fox), pp. 301–304. London, UK: Academic Press.
- Bell, A. S., de Roode, J. C., Sim, D. & Read, A. F. 2006 Within-host competition in genetically diverse malaria infections: parasite virulence and competitive success. *Evol. Int. J. Org. Evol.* **60**, 1358–1371.
- Bruce, M. C. & Day, K. P. 2002 Cross-species regulation of malaria parasitaemia in the human host. *Curr. Opin. Microbiol.* **5**, 431–437. (doi:10.1016/S1369-5274(02)00348-X)
- Bruce, M. C., Donnelly, C. A., Alpers, M. P., Galinski, M. R., Barnwell, J. W., Walliker, D. & Day, K. P. 2000 Cross-species interactions between malaria parasites in humans. *Science* **287**, 845–848. (doi:10.1126/science.287.5454.845)
- Chotivanich, K., Udomsangpetch, R., Simpson, J. A., Newton, P., Pukrittayakamee, S., Looareesuwan, S. & White, N. J. 2000 Parasite multiplication potential and the severity of falciparum malaria. *J. Infect. Dis.* **181**, 1206–1209. (doi:10.1086/315353)
- Chotivanich, K., Udomsangpetch, R., Pattanapanyasat, K., Chierakul, W., Simpson, J., Looareesuwan, S. & White, N. 2002 Hemoglobin E: a balanced polymorphism protective against high parasitemias and thus severe *P. falciparum* malaria. *Blood* **100**, 1172–1176.
- Cox, F. E. G. 1988 Major animal models in malaria research: rodent. In *Malaria: principles and practice of malarology* (eds W. H. Wernsdorfer & I. McGregor), ch. 49, 1503–1543. London, UK: Churchill Livingstone.
- Cromer, D., Evans, K. J., Schofield, L. & Davenport, M. P. 2006 Preferential invasion of reticulocytes during late-stage *Plasmodium berghei* infection accounts for reduced circulating reticulocyte levels. *Int. J. Parasitol.* **36**, 1389–1397. (doi:10.1016/j.ijpara.2006.07.009)
- de Roode, J. C. 2005 Within-host competition and the evolution of malaria parasites. PhD thesis, University of Edinburgh.
- de Roode, J. C., Culleton, R., Cheesman, S. J., Carter, R. & Read, A. F. 2004 Host heterogeneity is a determinant of

- competitive exclusion or coexistence in genetically diverse malaria infections. *Proc. R. Soc. B* **271**, 1073–1080. (doi:10.1098/rspb.2004.2695)
- de Roode, J. C. *et al.* 2005a Virulence and competitive ability in genetically diverse malaria infections. *Proc. Natl Acad. Sci. USA* **102**, 7624–7628. (doi:10.1073/pnas.0500078102)
- de Roode, J. C., Helinski, M. E. H., Anwar, M. A. & Read, A. F. 2005b Dynamics of multiple infection and within-host competition in genetically diverse malaria infections. *Am. Nat.* **166**, 531–542. (doi:10.1086/491659)
- Dietz, K., Raddatz, G. & Molineaux, L. 2006 Mathematical model of the first wave of *Plasmodium falciparum* asexual parasitemia in non-immune and vaccinated individuals. *Am. J. Trop. Med. Hyg.* **75**, 46–55.
- Duraisingh, M. T., Maier, A. G., Triglia, T. & Cowman, A. F. 2003 Erythrocyte-binding antigen 175 mediates invasion in *Plasmodium falciparum* utilizing sialic acid-dependent and -independent pathways. *Proc. Natl Acad. Sci. USA* **100**, 4796–4801. (doi:10.1073/pnas.0730883100)
- Field, J. W. 1949 Blood examination and prognosis in acute falciparum malaria. *Trans. R. Soc. Trop. Med. Hyg.* **43**, 33–48. (doi:10.1016/0035-9203(49)90022-X)
- Field, J. W. & Niven, J. C. 1937 A note on prognosis in relation to parasite counts in acute subtertian malaria. *Trans. R. Soc. Trop. Med. Hyg.* **6**, 569–574. (doi:10.1016/S0035-9203(37)90070-1)
- Frank, S. A. 1999 A model for the sequential dominance of antigenic variants in African trypanosome infections. *Proc. R. Soc. B* **266**, 1397–1401. (doi:10.1098/rspb.1999.0793)
- Gandon, S., Mackinnon, M. J., Nee, S. & Read, A. F. 2001 Imperfect vaccines and the evolution of pathogen virulence. *Nature* **414**, 751–776. (doi:10.1038/414751a)
- Garnham, P. C. C. 1966 *Malaria parasites and other haemosporidia*. London, UK: Blackwell Scientific Publishers.
- Gravenor, M. B., McLean, A. R. & Kwiatkowski, D. 1995 The regulation of malaria parasitaemia: parameter estimates for a population model. *Parasitology* **110**(Pt 2), 115–122.
- Haydon, D. T., Matthews, L., Timms, R. & Colegrave, N. 2003 Top-down or bottom-up regulation of intra-host blood-stage malaria: do malaria parasites most resemble the dynamics of prey or predator? *Proc. R. Soc. B* **270**, 289–298. (doi:10.1098/rspb.2002.2203)
- Hellriegel, B. 1992 Modelling the immune response to malaria with ecological concepts: short-term behaviour against long-term equilibrium. *Proc. R. Soc. B* **250**, 249–256. (doi:10.1098/rspb.1992.0156)
- Hetzel, C. & Anderson, R. M. 1996 The within-host cellular dynamics of bloodstage malaria—theoretical and experimental studies. *Parasitology* **113**, 25–38.
- Hutagalung, R., Wilairatana, P., Looareesuwan, S., Brittenham, G. M., Aikawa, H. & Gordeuk, V. R. 1999 Influence of hemoglobin E trait on the severity of falciparum malaria. *J. Infect. Dis.* **179**, 283–286. (doi:10.1086/314561)
- Jakeman, G. N., Saul, A., Hogarth, W. L. & Collins, W. E. 1999 Anaemia of acute malaria infections in non-immune patients primarily results from destruction of uninfected erythrocytes. *Parasitology* **119**(Pt 2), 127–133. (doi:10.1017/S0031182099004564)
- Kitchen, S. F. 1949a Falciparum malaria. In *Malariaology* (ed. M. F. Boyd), pp. 995–1016. London, UK: Saunders.
- Kitchen, S. F. 1949b Symptomatology: general considerations. In *Malariaology* (ed. M. F. Boyd), pp. 966–994. London, UK: Saunders.
- Mackey, M. C. 1996 Mathematical models of hematopoietic cell replication and control. In *The art of mathematical modeling: case studies in ecology, physiology and biofluids* (eds H. G. Othmer, F. R. Adler, M. A. Lewis & J. C. Dallon), pp. 149–178. New York, NY: Prentice-Hall.
- Mackinnon, M. J. & Read, A. F. 2004 Virulence in malaria: an evolutionary viewpoint. *Phil. Trans. R. Soc. B* **359**, 965–986. (doi:10.1098/rstb.2003.1414)
- Mary, J. Y., Valleron, A. J., Croizat, H. & Frindel, E. 1980 Mathematical analysis of bone marrow erythropoiesis: application to C3H mouse data. *Blood Cells* **6**, 241–262.
- Mason, D. P., McKenzie, F. E. & Bossert, W. H. 1999 The blood-stage dynamics of mixed *Plasmodium malariae*–*Plasmodium falciparum* infections. *J. Theor. Biol.* **198**, 549–566. (doi:10.1006/jtbi.1999.0932)
- McQueen, P. G. & McKenzie, F. E. 2004 Age-structured red blood cell susceptibility and the dynamics of malaria infections. *Proc. Natl Acad. Sci. USA* **101**, 9161–9166. (doi:10.1073/pnas.0308256101)
- McQueen, P. G. & McKenzie, F. E. 2006 Competition for red blood cells can enhance *Plasmodium vivax* parasitemia in mixed-species malaria infections. *Am. J. Trop. Med. Hyg.* **75**, 112–125.
- Menendez, C., Fleming, A. F. & Alonso, P. L. 2000 Malaria-related anaemia. *Parasitol. Today* **16**, 469–476. (doi:10.1016/S0169-4758(00)01774-9)
- Miller, L. H., Baruch, D. I., Marsh, K. & Doumbo, O. K. 2002 The pathogenic basis of malaria. *Nature* **415**, 673–679. (doi:10.1038/415673a)
- Molineaux, L., Diebner, H. H., Eichner, M., Collins, W. E., Jeffery, G. M. & Dietz, K. 2001 *Plasmodium falciparum* parasitaemia described by a new mathematical model. *Parasitology* **122**, 379–391. (doi:10.1017/S0031182001007533)
- Mota, M. M., Brown, K. N., Holder, A. A. & Jarra, W. 1998 Acute *Plasmodium chabaudi chabaudi* malaria infection induces antibodies which bind to the surfaces of parasitized erythrocytes and promote their phagocytosis by macrophages *in vitro*. *Infect. Immun.* **66**, 4080–4086.
- Perelson, A. S. 2002 Modelling viral and immune system dynamics. *Nat. Rev. Immunol.* **2**, 28–36. (doi:10.1038/nri700)
- Phillips, A. N. 1996 Reduction of HIV concentration during acute infection: independence from a specific immune response. *Science* **271**, 497–499. (doi:10.1126/science.271.5248.497)
- Phillips, R. S., Brannan, L. R., Balmer, P. & Neuville, P. 1997 Antigenic variation during malaria infection—the contribution from the murine parasite *Plasmodium chabaudi*. *Parasite Immunol.* **19**, 427–434. (doi:10.1046/j.1365-3024.1997.d01-239.x)
- Recker, M., Nee, S., Bull, P. C., Kinyanjui, S., Marsh, K., Newbold, C. & Gupta, S. 2004 Transient cross-reactive immune responses can orchestrate antigenic variation in malaria. *Nature* **429**, 555–558. (doi:10.1038/nature02486)
- Regoes, R. R., Antia, R., Garber, D. A., Silvestri, G., Feinberg, M. B. & Stavrakas, S. I. 2004 Roles of target cells and virus-specific cellular immunity in primary simian immunodeficiency virus infection. *J. Virol.* **78**, 4866–4875. (doi:10.1128/JVI.78.9.4866-4875.2004)
- Simpson, J. A., Silamut, K., Chotivanich, K., Pukrittayakamee, S. & White, N. J. 1999 Red cell selectivity in malaria: a study of multiple-infected erythrocytes. *Trans. R. Soc. Trop. Med. Hyg.* **93**, 165–168. (doi:10.1016/S0035-9203(99)90295-X)
- Suzuki, M., Ohneda, K., Hosoya-Ohmura, S., Tsukamoto, S., Ohneda, O., Philipsen, S. & Yamamoto, M. 2006 Real-time monitoring of stress erythropoiesis *in vivo* using Gata1- and beta-globin LCR-luciferase transgenic mice. *Blood* **108**, 726–733. (doi:10.1182/blood-2005-10-4064)